# Chapter-1

## Introduction and Scope of the Thesis

## 1.1 Photodetectors

Photodetectors, also known as photosensors or light detectors, have been a critical component in a wide range of applications including imaging, optical communication, scientific research, environmental monitoring and industrial automation. Efficient and high-speed data transmission in the form of an optical signal is a critical requirement in today's information and communication technology era. Since electronic circuits and systems can only process electrical signals, optical signals must be converted into electrical signals for various applications. Photodetectors are semiconductor optoelectronic devices that convert optical signals (photons) into measurable electrical signals, typically in the form of current or voltage [1], [2]. The basic operating principle of photodetectors is based on the phenomena known as the *photoelectric effect*. This process occurs through the following sequential steps:

(i) **Photon Incidence:** The optical signals consisting of photons are allowed to incident on the surface of the photodetector device**.**

(ii) **Photon Absorption and Charge Carrier Generation:** The incident photons are absorbed by the active semiconductor material of the photodetector. Photons with energy greater than the bandgap of the semiconductor excite electrons from the valence band (VB) to the conduction band (CB), thereby generating an electron-hole (e–h) pair for each absorbed photon.

(iii) **Carrier Separation and Charge Carrier Transportation:** The electrons and holes of the photogenerated electron-hole pairs are separated by an electric field created by an externally applied bias voltage to the device. The electrons drift in the direction

opposite to the electric field, while the holes drift in the same direction, resulting in the separation of charge carriers.

(iv) **Electrical Signal Generation:** These charge carriers are collected at their respective electrodes to produce a measurable electric current or voltage. Since the incident photon flux density is proportional to the intensity of the light falling on the photodetector, the resulting photocurrent is also proportional to the intensity of the incident light.

**Figure 1.1** illustrates various applications of photodetectors in optical communication systems, healthcare monitoring, environmental monitoring, smart electronic devices, food production performance evaluation, security and defense, as well as imaging and remote sensing systems [3]–[9]. In recent years, the emergence of innovative technologies such as Artificial Intelligence (AI) and the Internet of Things (IoT) has further expanded the scope and applicability of photodetectors.

Different materials are used in photodetectors to enable their operation across various spectral regions, namely the ultraviolet (UV, <400 nm), visible (Vis, 400–700 nm), and infrared (IR, >700 nm) ranges. The present thesis focuses on exploring the relatively less studied $MoSe_2$ thin films for the development of broadband photodetectors operating in the UV–Vis or UV–Vis–NIR regions.

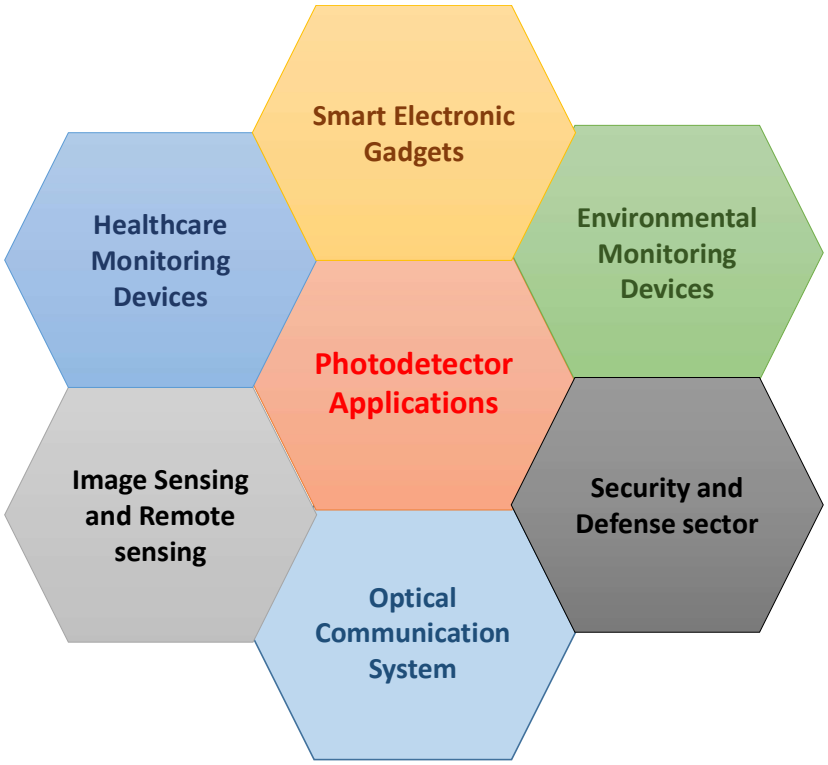


**Figure 1.1** Application of Photodetectors in different field of Electronics.

The outline of this chapter is described as follows: Section 1.2 introduces the classification of photodetectors based on their device structure and operating wavelength regions. In Section 1.3, we define some basic performance parameters of photodetectors. Section 1.4 focus on material selection for photodetector application. Section 1.5 introduces Transition Metal Dichalcogenides (TMDs) for Photodetectors. In Section 1.6, we have mentioned some synthesis techniques for TMD materials. Section 1.7 describes thin film deposition and characterization techniques. In Section 1.8, Literature review on TMDs has been presented. Section 1.9 and 1.10 describes Thesis motivation and Thesis objective respectively. And lastly, Section 1.11 presents the organization of the thesis.

## 1.2 Classification of Photodetectors

Photodetectors may be classified based on their physical structures as well as their spectral response characteristics, as discussed below.

### 1.2.1. Classification based on Physical Structure

Based on their physical structures, photodetectors are broadly classified into three types: photoconductors, photodiodes, and phototransistors. These are briefly discussed below.

**1. Photoconductive Photodetectors or Photoconductors:**

The basic structure of a photoconductive-type photodetector is shown in **Figure 1.2** (a). It typically consists of a piece of semiconductor material (serving as the photoactive region) with two ohmic contacts (electrodes) placed on its surface at a certain distance apart. Under dark conditions, the semiconductor maintains a high resistivity. However, when the device is illuminated with light whose photon energy exceeds the semiconductor's bandgap, electron-hole pairs are generated through the photoelectric effect. This leads to an increase in conductivity (i.e., a decrease in resistivity) of the semiconductor.

When a voltage is applied across the electrodes, the change in conductivity results in a corresponding change in the current flowing through the device. The resulting photocurrent—defined as the difference between the current under illumination and that in the dark—is proportional to the intensity of the incident light.

Photoconductive photodetectors are structurally simple and widely used in applications such as light sensors, infrared detectors, and optical switches [2]. However, their use in optical

communication and computing is somewhat limited due to their inherently slow response speed [10], [11].

## 2. Photodiodes:

Photodiodes are essentially two-terminal devices based on either p–n junction diodes or Schottky diodes, operated under reverse bias conditions [2]. A schematic of a vertical photodiode device is shown in **Figure 1.2** (b). Under dark conditions, the current is primarily the reverse saturation current, which is very small. When the reverse-biased p–n junction is illuminated, electron–hole pairs are generated in the depletion region via the photoelectric effect. These carriers are rapidly separated and swept out of the depletion region by the strong internal electric field, resulting in a photocurrent. This photocurrent is proportional to the intensity of the incident light.

The response speed of large-area photodiodes is typically limited by increased recombination of photogenerated carriers in the neutral regions. To mitigate this, PIN photodiodes—which incorporate an intrinsic semiconductor layer between the p-type and n-type regions—are often preferred [2], [12] . Another widely used structure is the avalanche photodiode (APD), which operates under a high reverse bias. This high field causes impact ionization, leading to avalanche multiplication and a significantly enhanced photocurrent. Such devices are well-suited for applications requiring high sensitivity and fast response [2], [12].

In addition to conventional p–n junctions, Schottky photodiodes are also commonly used, particularly for high-speed applications [1], [2]. Furthermore, metal–semiconductor–metal (MSM) photodiodes, which utilize two Schottky junctions, are also employed in various optoelectronic systems [1], [13].

### 3. Phototransistors:

Phototransistors are three-terminal devices—typically referred to as the emitter, base, and collector as shown in **Figure 1.2** (c). Unlike conventional transistors, phototransistors use light instead of an electrical bias at the base to control the flow of current. When light illuminates the base region, electron–hole pairs are generated through the photoelectric effect, resulting in a small base current. This, in turn, activates the transistor and produces a significantly larger collector current due to the inherent current amplification capability of the device [2].

Phototransistors are particularly useful in opto-couplers, where electrical isolation is important. However, they are generally not used in optical communication systems due to their slower response speed compared to conventional photodiodes. This limitation arises primarily from their inherently large active area, which increases carrier transit time. Additionally, the fabrication of phototransistors is more complex than that of photodiodes [2].

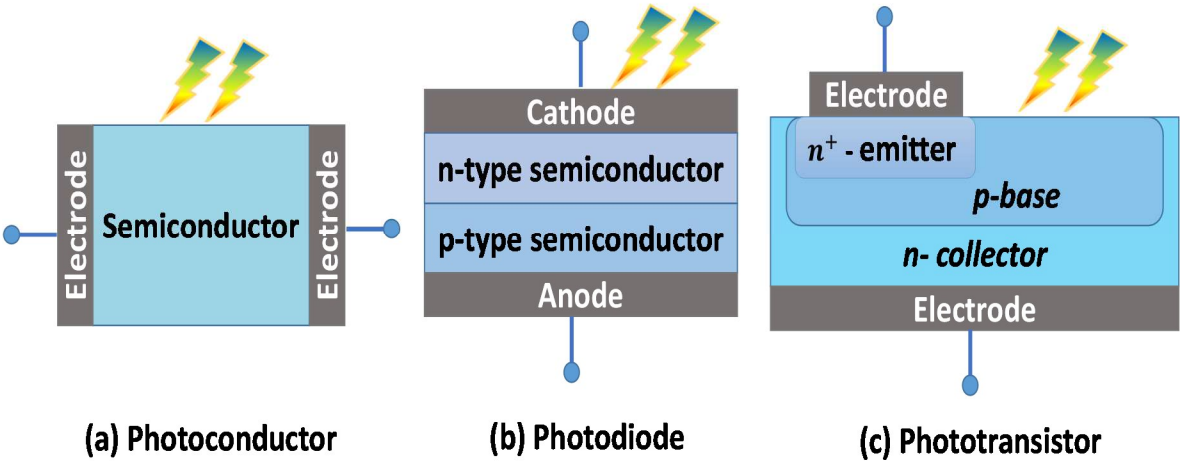


**Figure 1.2** Photodetector classification on the basis of their Physical Structure.

### 1.2.2. Clasification based on Spectral Response

Based on the wavelength dependent photoresponse characteristics, photodetectors can be classified as follows:

1. **Ultraviolet Photodetectors**:

   The active material of the ultraviolet (UV) photodetectors or **UV detectors** selected to absorb the ultraviolet radiation (wavelengths typically between 10 nm and 400 nm). Commonly used UV detectors are used to detect UV radiation spanning from ~**200 nm to ~400 nm**. UV detectors are widely used for flame detection and combustion monitoring [14], solar UV radiation and ozone monitoring [15], UV sterilization monitoring [16], environmental pollution monitoring [17], missile launch and space Applications [2], wearable UV monitoring devices application [18] etc.

2. **Visible Photodetectors:**

   These type of photodetectors are designed to detect light in the **visible spectrum** (**400–700 nm**). They are widely used in imaging and digital cameras [19], biomedical imaging and fluorescence detection [20], ambient light sensing in consumer electronics (e.g. smartphones, laptops, and TVs to adjust their screen brightness automatically) [21], machine vision and industrial automation [22], remote sensing and satellite imaging [23], optical communication (Short-range, Visible Light Communication (VLC)) [24] etc.

**3. Infrared Photodetectors:**

**Infrared (IR) photodetectors** are developed to detect light with wavelengths above 700 nm. The IR photodetectors are used in thermal imaging and night vision [25] , space and earth observation [26], gas and chemical sensing (e.g. $CO_2$, $CH_4$, NOx, etc.) using non-dispersive infrared (NDIR) spectroscopy [27], optical fiber and free-space IR Communication [28] etc.

**4. Narrowband Photodetectors:**

**Narrowband photodetectors** are designed to detect light within a very specific and narrow spectral range (typically with a full-width-at-half-maximum (FWHM) of 10–30 nm or less). They are used in multispectral and hyperspectral imaging [29], biomedical diagnostics and biosensing [30], selective optical communication (e.g. Wavelength-Division Multiplexing, VLC) [31] etc.

**5. Broadband Photodetector:**

**Broadband photodetectors** are used for the detection of light with a wide spectral range from UV through visible to IR. These type photodetectors are used in optical coherence tomography (OCT) [32], solar energy and photovoltaics characterization [33], spectroscopy and hyperspectral imaging [34], free-space optical communication [28] etc.

Various types of photodetectors classified on their spectral response characteristics are summarized in **Figure 1.3**.

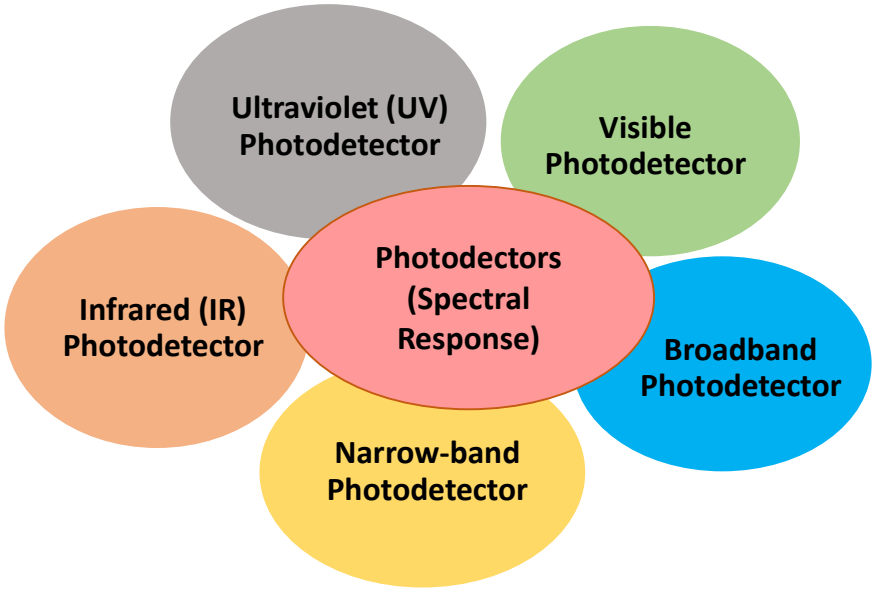


**Figure 1.3** Photodetector classification on the basis of their Spectral response.

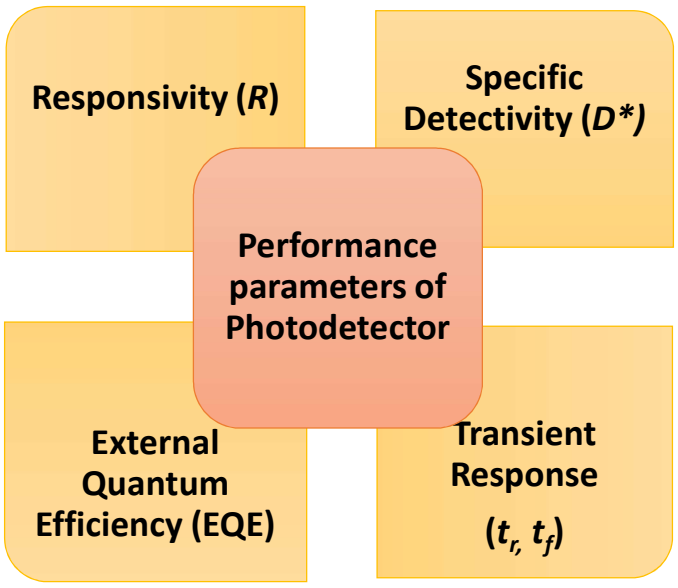


**Figure 1.4** Performance parameters of the Photodetector.

## 1.3 Performance Parameters of the Photodetector

The key parameters which are essential to determine the performance metrics of any photodetector are shown in the **Figure 1.4**. They are briefly discussed in the following:

### 1.3.1. Responsivity (*R*):

Responsivity of a photodetector defines its effectiveness in converting incident optical power into an electrical signal (typically current or voltage). It quantifies how much output (current or voltage) is generated per unit of incident light power [6], [8], [35]. It may be expressed as

$$R(\lambda) = \frac{(I_{light} - I_{dark})/A_{eff}}{P_{opt}(\lambda)/A_{eff}} = \frac{(I_{light} - I_{dark})}{P_{opt}(\lambda)} \quad (\text{A/W}) \tag{1.1}$$

where, $I_{light}$ is the current generated by incident optical power, $P_{opt}(\lambda)$ is incident optical power at wavelength $\lambda$, $I_{dark}$ is current under the dark condition of the device, $A_{eff}$ is effective area of the device and $(I_{light} - I_{dark})$ represents the photocurrent produced by the photodetector.

### 1.3.2. Specific Detectivity (*D**):

Specific detectivity (D*) is an important figure of merit for photodetectors. It quantifies their ability to detect weak optical signals, normalized for detector area and bandwidth. It is especially useful for comparing the performance of detectors of different sizes and materials. Mathematically, it can be expressed as [36], [37]

$$D^*(\lambda) = R(\lambda) \times \sqrt{\frac{A_{eff}}{2 \times e \times I_{dark}}} \text{ Jones} \quad (1.2)$$

where $R(\lambda)$ is the responsivity at wavelength $\lambda$, $A_{eff}$ is the effective area of the device; $e$ is the charge of an electron; and $I_{dark}$ is the dark current.

### 1.3.3. External Quantum Efficiency (EQE):

External Quantum Efficiency (EQE) is defined as the ratio of total number of electron-hole pairs collected by the electrodes per second to the incident number of incident photons at wavelength $\lambda$ striking its surface per second [9], [38], [39]. It is mathematically expressed as

$$\text{EQE (\%)} = 1240 * \frac{R(\lambda)}{\lambda} * 100 \quad (1.3)$$

where R is the responsivity; λ is the wavelength of the light incident on the device.

The EQE is typically expressed as a percentage (%). In general, EQE is less than 100% if there are no avalanche or internal gain mechanisms in the detector. An EQE of 100% means one electron is collected for each photon absorbed and EQE > 100% is possible in avalanche photodiodes or internal gain detectors due to carrier multiplication.

### 1.3.4. Transient Response Times: Rise Time and Fall Time:

The **transient response** characteristics of a **photodetector** are carried out to estimate response speed of the device. The response speed (or temporal response) of a photodetector refers to how quickly it can respond to changes in the incident light signal. It determines the

detector's maximum operating frequency or bandwidth, which is crucial for high-speed optical communication and fast sensing applications. The response speed is often quantified by rise time $(t_r)$ and $(t_f)$. The rise time is defined as the time taken for the output photocurrent to rise from 10% to 90% of its maximum value whereas the fall time is the time taken for the output to fall from 90% to 10% of its peak value [39], [40]. While the rise time can give an idea about the bandwidth of the detector, the fall time determines how quickly a detector can be reset and get ready for detecting the next optical signal pulse. The 3-dB bandwidth of the photodetector is approximately expressed in term of $t_r$ as [2]

$$f_{3-d} \approx \frac{0.35}{t_r} \tag{1.4}$$

## 1.4 Material Selection for Photodetection Application

The proper selection of materials for photodetectors is a critical step in achieving the desired efficiency, sensitivity, speed, and spectral range. The electronic bandgap energy $(E_g)$ of a semiconductor is a key parameter in determining the spectral response of a photodetector. It is well known that photoexcited electron-hole pairs are generated via the photoelectric effect when the incident photon energy $\left(E_{ph} = \frac{hc}{\lambda}\right)$ is equal to or greater than the bandgap energy i.e. $\left(E_{ph} = \frac{hc}{\lambda}\right) \geq E_g$.

Material selection depends on both the absorption characteristics and the desired spectral range of operation. In general, wide bandgap materials $\left(E_g > 3.0 \text{ eV}\right)$ are used for ultraviolet

(UV) detection, materials with moderate bandgaps $(E_g \sim 1.5 - 3.0\ \text{eV})$ are suitable for visible light detection, and narrow bandgap materials $(E_g < 1.5\ \text{eV})$ are typically chosen for infrared (IR) photodetectors**.**

The active materials used in photodetector design should exhibit high carrier mobility and lifetime, low intrinsic carrier concentration, and low defect density. In addition, they should offer high thermal stability, compatibility with silicon-based CMOS technology for smart device integration, low toxicity and environmental friendliness, low cost, wide availability, and high absorption coefficients in the desired spectral region. High absorption is particularly beneficial for enabling thinner active layers, reducing carrier transit time, and improving device speed [2], [41].

Some commonly used semiconductors for various photodetector applications are listed in **Table 1.1**. It is important to note that metal oxides are widely used in UV photodetectors while Transition Metal Dichalcogenide (TMD) materials are used in Visible-NIR photodetectors. Thus, the combination of metal oxides and TMDs can be explored for wideband photodetectors covering UV-Visible or UV-Visible-NIR regions.

**Table 1.1** Some commonly used materials for photodetectors

| Material | Bandgap (eV) | Spectral Range | Type | Key Feature |
|---|---|---|---|---|
| Si | 1.12 | Visible (Vis)–Near Infrared (NIR) | Elemental | CMOS compatible |
| InGaAs | 0.75–1.35 | NIR | III–V | Telecom & high quantum efficiency (QE) |
| GaAs | 1.42 | Vis–NIR | III–V | High-speed |
| Ge | 0.66 | NIR | Elemental | Ge-on-Si detectors |
| HgCdTe | Tunable | IR | II–VI | IR imaging, high sensitivity |
| ZnO, $TiO_2$ | >3.0 | UV | Metal Oxide | UV sensors, eco-friendly |
| Graphene | 0 | Broadband | Two Dimensional (2D) Material | Ultrafast, broadband |
| $MoS_2$, $MoSe_2$, $WS_2$ | ~1–2 | Vis–NIR | 2D Transition Metal Dichalcogenide (TMD) Material | Flexible photodetectors |
| PbS QDs | Tunable | Vis–NIR | Quantum Dot | Printable, tunable |
| Perovskites | ~1.5 | Vis–NIR | Hybrid | High QE, low-cost |
| Organic Polymers | ~1.5–2.5 | Vis–NIR | Organic semiconductors | Flexible, low-cost |

## 1.5 Transition Metal Dichalcogenides (TMDs) for Photodetectors

Transition Metal Dichalcogenides (TMDs) are well-known members of the two-dimensional (2D) material family. Over the past few years, 2D materials and their device applications have attracted significant attention from researchers in the field of optoelectronics [5], [42]. Although TMDs have been known for decades, they gained renewed interest only after the discovery of graphene—the first 2D material in 2004 [43], [44]. This milestone sparked a

surge of research activity in exploring other 2D materials, among which TMDs have drawn immense interest due to their exceptional electronic and optical properties.

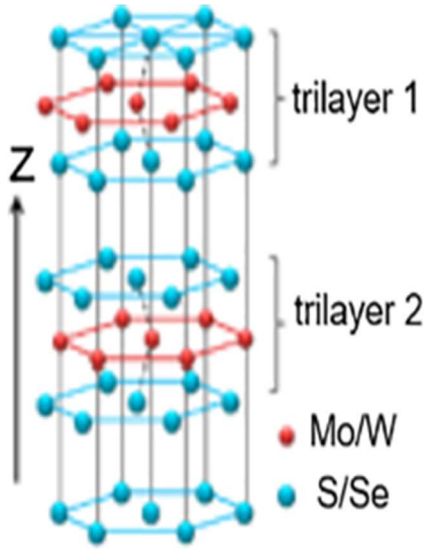


**Figure 1.5** Schematic reprenstation of Crystal structure of TMDs

Today, TMDs are among the most extensively studied materials for applications in solid-state devices, energy storage, optoelectronics, and photo-electrocatalysis [5], [45]–[49]. Structurally, TMDs exist primarily in two phases: trigonal prismatic (2H) and octahedral (1T) coordination of transition metal atoms. As a result, TMDs exhibit a wide range of electronic behaviors—from insulating to metallic to semiconducting. The 2H phase typically shows semiconducting properties, while the 1T phase exhibits metallic behavior [5], [43]. TMDs are generally represented by the formula $MX_2$, where M stands for a transition metal (e.g., Mo, W), and X denotes a chalcogen (e.g., S, Se, Te). They possess a layered architecture in which a single layer of transition metal atoms is sandwiched between two layers of chalcogen atoms [50]–[54]. As illustrated in the schematic **Figure 1.5**, atoms within

each layer are held together by strong covalent bonds, whereas the adjacent layers are bonded via weak van der Waals forces [43], [52]–[55]. This allows TMDs to be easily exfoliated down to monolayers.

One of the remarkable features of TMDs is that their semiconducting behavior undergoes a transition from an indirect to a direct bandgap when scaled down from the bulk to monolayer form [5], [42], [51]**.** This layer-dependent bandgap engineering makes them highly promising candidates for optoelectronic device applications [5], [43], [51]**.**

TMD-based photodetectors have been extensively studied in recent years. These materials are considered excellent candidates for broadband, highly sensitive, and flexible photodetection systems due to their strong light absorption and ultrathin geometry [56]–[59]**.** Compared to graphene, TMDs offer longer carrier lifetimes, making them more suitable for high-performance photodetectors[59]–[61]**.**

Among TMDs, $MoS_2$ is perhaps the most widely studied, while $MoSe_2$ has been relatively less explored. However, $MoSe_2$ offers several advantages over $MoS_2$, including higher electrical conductivity and light absorption capacity [61]**,** higher carrier mobility [62], superior photodetection responsivity [63], fast response times [63], [64], and enhanced photocatalytic activity [65]. That is why, there are enough scopes for exploring $MoSe_2$ for photodetection applications.

## 1.6 Synthesis Techniques for TMD Materials

Synthesis of high quality TMD materials is essential for device fabrication. TMD materials can be synthesized by several techniques such as the Chemical Vapor Deposition (CVD) [62], [66], Mechanical Exfoliation [58], [67], Liquid Phase Exfoliation [68], [69] and Solvothermal synthesis methods as shown in **Figure 1.6**. They are briefly discussed in the following.

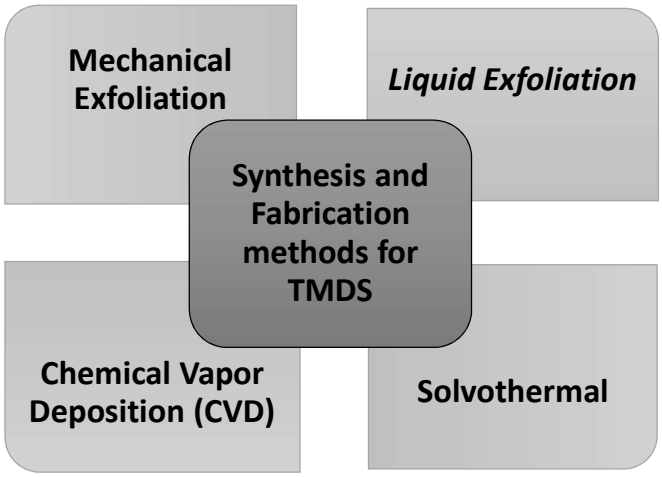


**Figure 1.6** Synthesis and Fabrication methods for TMDs.

### 1.6.1. Chemical Vapor Deposition (CVD):

Chemical Vapor Deposition (CVD) is a widely used technique for the synthesis of high-quality thin films and nanomaterials, particularly two-dimensional (2D) materials like graphene and transition metal dichalcogenides (TMDs) [54], [70], [71]. In CVD, gaseous precursors react or decompose on a heated substrate surface under controlled temperature and pressure conditions, enabling the formation of uniform and crystalline layers with precise

control over thickness, morphology, and composition. By tuning parameters such as temperature, gas flow rates, and precursor ratios, CVD allows for scalable fabrication of large-area, high-purity films suitable for electronic, optoelectronic, and catalytic applications. This method has been instrumental in advancing the production of 2D materials with excellent structural and electronic properties, facilitating their integration into next-generation devices.

### 1.6.2. Mechanical Exfoliation Method:

Mechanical Exfoliation Method (also known as the Scotch Tape Method) is a simple and widely used technique to isolate atomically thin layers—particularly monolayer or few-layer 2D materials, such as graphene, $MoS_2$, and other transition metal dichalcogenides (TMDs)—from their bulk crystals. In this method, a bulk crystal (e.g., graphite or $MoS_2$) is placed on adhesive tape, which is repeatedly folded and peeled apart to thin the flakes. The tape is then pressed onto a clean substrate (e.g., a $Si/SiO_2$ wafer), transferring some flakes—potentially including monolayers or few-layer flakes—onto the substrate.

### 1.6.3. Liquid-Phase Exfoliation:

The Liquid Phase Exfoliation (LPE) is a widely used, scalable method for producing two-dimensional (2D) nanosheets—such as graphene, $MoS_2$, $WS_2$, and other transition metal dichalcogenides (TMDs)—from their bulk layered crystals [51], [72]. In this technique, bulk powder or crystals are dispersed in a suitable solvent or a surfactant-assisted aqueous solution. The dispersion is then subjected to ultrasonication, which generates cavitation

forces strong enough to overcome the weak van der Waals interactions between the layers, leading to the exfoliation of the material into monolayer or few-layer nanosheets suspended in the liquid. After sonication, the mixture is centrifuged to remove unexfoliated particles and to separate flakes based on their thickness and size. The supernatant contains exfoliated 2D nanosheets that can be collected for further use. This method is highly advantageous for its simplicity, cost-effectiveness, and compatibility with large-scale production. It enables the formulation of 2D material-based inks, which are useful for printable electronics and flexible devices. However, LPE often results in a broad distribution of flake sizes and thicknesses, and the ultrasonication process may introduce defects into the crystal structure. Additionally, residual solvents or surfactants can affect the purity and electronic performance of the materials. Despite these limitations, LPE remains a popular choice for applications in energy storage, catalysis, sensing, and thin-film fabrication due to its versatility and scalability [50], [72].

### 1.6.4. Solvothermal Synthesis:

**Solvothermal synthesis** is a widely employed technique for fabricating nanostructured materials, including two-dimensional (2D) materials, under high-temperature and high-pressure conditions in a sealed autoclave using organic solvents [43], [73], [74]. In this method, suitable precursors are dissolved in a solvent and then heated, typically between 100°C and 300°C, to facilitate nucleation and controlled crystal growth. By adjusting parameters such as temperature, reaction time, solvent type, and precursor concentration, the morphology, size, and crystallinity of the resulting nanomaterials can be precisely tuned.

Solvothermal synthesis has been successfully applied to prepare various transition metal dichalcogenides (TMDs), metal oxides, and hybrid nanostructures with uniform composition and desirable properties for applications in catalysis, energy storage, and optoelectronics. Its ability to produce high-quality materials with complex architectures makes it a valuable alternative to physical deposition methods. However, post-synthesis treatments are often necessary to achieve the desired material properties [48], [51], [54].

## 1.7 Thin Film Deposition and Characterization Techniques

Various steps of thin film device fabrication and characterizations are shown in **Figure 1.7**. After material synthesis, their thin films on the substrates are fabricated by depositing the materials using various thin film deposition techniques shown in **Figure 1.8**. Post deposition film treatment may be required to improve the quality of the thin films. Samples of thin films are sent for investigating their morphological, structural, electronic and optoelectronic properties. Once the desired film characteristics are obtained, metal electrode contacts are fabricated on the thin films for device characterization.

Among various thin film deposition techniques shown in **Figure 1.8** before proceeding for the device characterization, various electronic and optoelectronic properties of the films are measured. The fabrication of thin film devices starts with materials synthesis followed by their deposition. Various synthesis techniques of TMDs were described briefly in the last section. The present thesis considers the $MoSe_2$ as the main 2D photoactive TMD material for fabricating some broadband photodetectors. To extend the broadband spectral response including the UV region, we have also combined ZnO colloidal quantum dots (CQDs) with

$MoSe_2$. While thin films from the synthesized $MoSe_2$ powder has been obtained by vacuum thermal evaporation method, the thin films of ZnO CQDs have been obtained by spin coating method. We have discussed briefly A complete device fabrication and characterization involves numerous sequential steps from material synthesis to final device parameters measurement. These steps as shown in **Figure 1.7** are as follows:

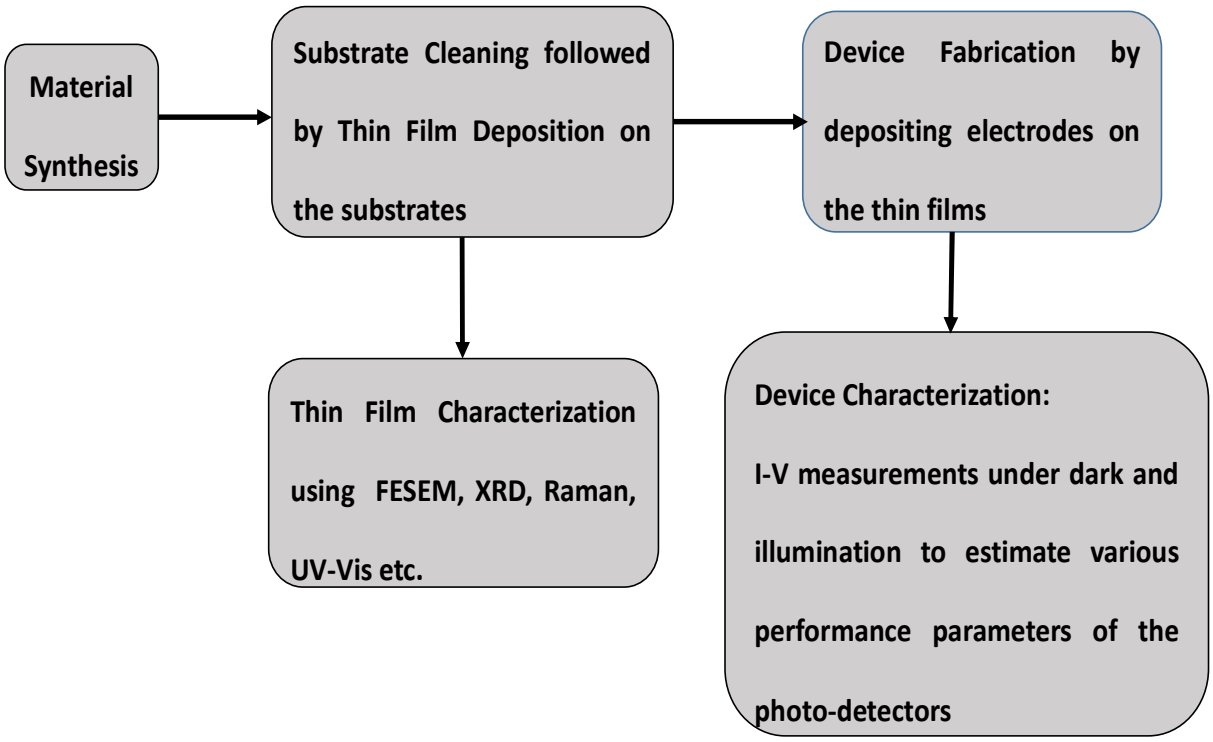


**Figure 1.7** Various steps involved in device fabrication and characterization.

### 1.7.1. Thin Film Deposition Methods

Among various thin film deposition techniques listed in **Figure 1.8**, only the Vacuum Thermal Deposition (VTD) and spin coating methods have been used for thin film preparation in the present thesis. They are briefly discussed below:

**Vacuum Thermal Deposition (VTD):** The Vacuum Thermal Deposition (VTD) is a widely used physical vapor deposition (PVD) technique for fabricating thin films by thermally evaporating materials in a high-vacuum environment [75]. In this process, the source material is heated—typically using a resistive filament or a crucible—until it evaporates, and the vaporized atoms travel through the vacuum and condense onto a cooler substrate to form a thin film. The high vacuum (typically in the range of $10^{-5}$ to $10^{-7}$ Torr) minimizes contamination and ensures a high-purity film. VTD is commonly employed for depositing metals, organic semiconductors, and some dielectrics, particularly in applications such as organic light-emitting diodes (OLEDs), solar cells, and microelectronic devices. While it offers advantages like simplicity, low cost, and good control over film thickness, it is generally limited to materials with low to moderate melting points and provides poor step coverage due to its line-of-sight deposition nature. Nevertheless, VTD remains a valuable method for fabricating uniform thin films, especially where material purity and low processing temperatures are critical.

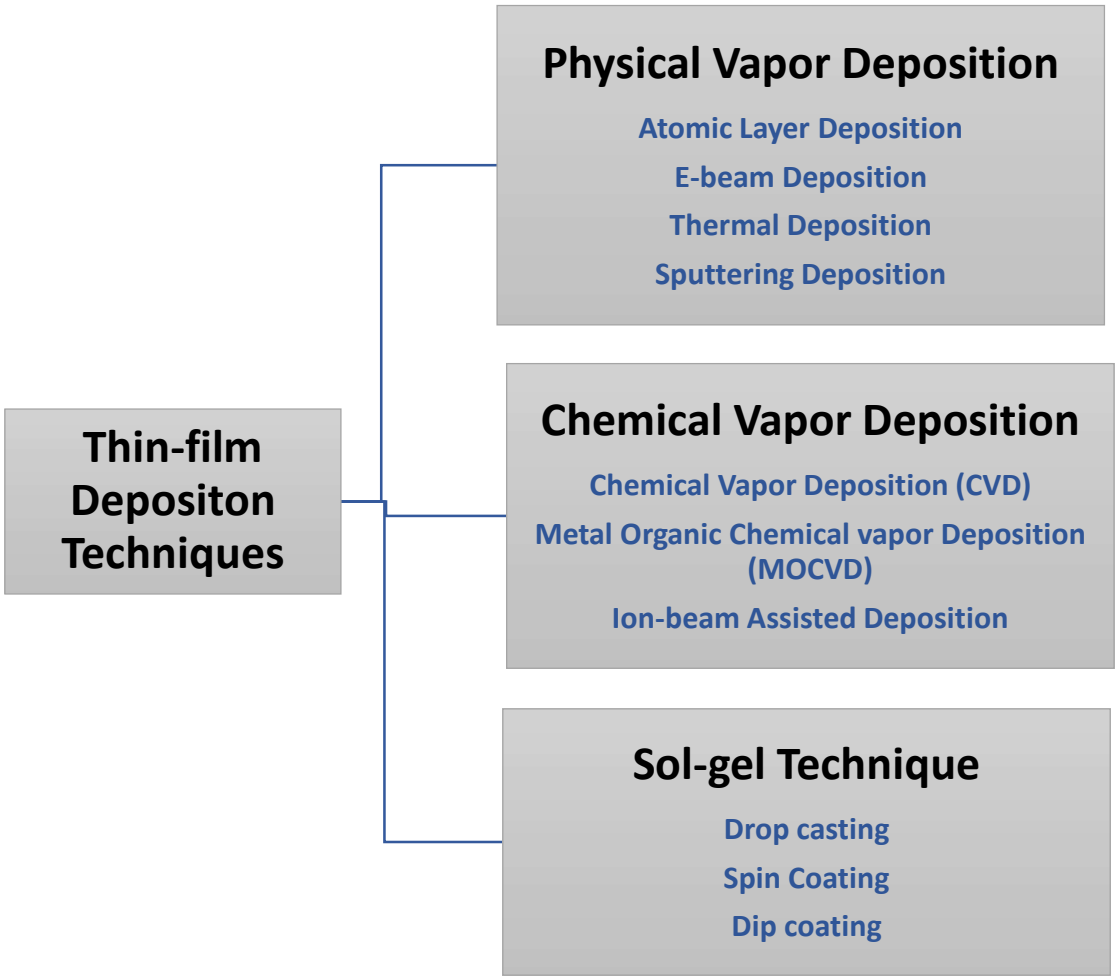


**Figure 1.8** Thin-film Deposition Techniques

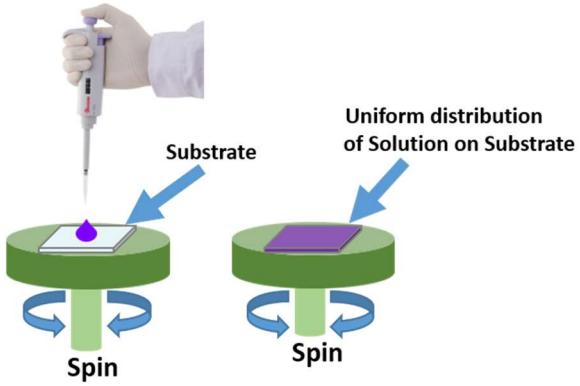


**Figure 1.9** Spin coating method of thin film deposition

**Spin Coating Method:** Spin coating is a widely used technique for depositing uniform thin films on flat substrates [76]. In this method, a small amount of liquid precursor solution is dispensed onto the center of a substrate, which is then rapidly rotated at high speeds (typically 1000–8000 rpm). It is demonstrated in **Figure 1.9**. The centrifugal force spreads the solution across the surface, while solvent evaporation during spinning results in the formation of a thin, uniform film. The final film thickness depends on several factors, including the spin speed, solution viscosity, and spinning duration. Spin coating is particularly advantageous due to its simplicity, cost-effectiveness, and ability to produce high-quality films with excellent uniformity over large areas. However, it is generally limited to flat substrates and materials that can be processed from solution**.**

### 1.7.2. Thin Film Characterization Techniques

After thin film deposition, various characterization techniques are performed on the deposited film. These are as follows:

#### 1.7.2.1. Material Characterization Techniques

The material characterization techniques include X-ray Diffraction (XRD), Raman Spectroscopy, and X-ray Photoelectron Spectroscopy (XPS).

**X-ray Diffraction (XRD)** is used to characterize powders, thin films, and crystals by providing information on lattice parameters, crystal structure, defects, and internal stress. It works by analyzing how X-rays interact with the atoms in the material, producing a diffraction pattern that reflects the atomic arrangement.

**Raman Spectroscopy** examines how light, typically from a laser, is inelastically scattered by a material. The resulting energy (or wavelength) shift reveals the vibrational modes of the atoms. It is a crucial tool for material identification, assessing crystallinity and defects, and studying strain, doping, and temperature effects.

**X-ray Photoelectron Spectroscopy (XPS)** is a surface-sensitive technique in which the sample is irradiated with X-rays (commonly Al Kα at 1486.6 eV), and the kinetic energy of emitted electrons is measured. From this, the binding energy of the electrons is calculated, providing a spectrum that reveals the elements present, their oxidation states, chemical environments, and the surface composition of the top ~5–10 nm of the material.

#### 1.7.2.2. Surface Characterization

To analyze the surface morphology of the deposited thin film at the nanoscale, Field-Emission Scanning Electron Microscopy (FE-SEM) is used. The Atomic Force Microscopy (AFM) is used to determine the surface roughness and height profile of the thin films.

### 1.7.3. Optoelectronic Characterizations:

After the material characterization, fabricated device is characterized for optical and optoelectronic characterizations. They are as follows:

#### 1.7.3.1. UV-Visible (UV-Vis) Spectroscopy:

For photodetector applications, optical characterization using a UV-Vis spectrometer is performed to determine the spectral region of maximum absorbance of the active material

used in the photodetector. The schematic and working mechanism representation of the UV-Vis Spectroscopy (V-770 from JASCO, Japan) measurement setup shown in **Figure 1.10** is used for thin-film characterization in our thesis work.

#### 1.7.3.2. Current-Voltage (I-V) measurements:

The electrical and optical characteristics of the fabricated photodetectors devices are measured using a semiconductor parameter analyzer ((Model: B1500A) system from Keysight, USA). The current–voltage (I–V) characteristics of the device are measured under both dark and illuminated conditions to evaluate the photocurrent under reverse bias operation. The difference between the dark and light current represents the photocurrent generated by the device. **Figure 1.11** shows measurement setup used to perform I-V characterization of the fabricated device in this thesis work.

#### 1.7.3.3. Photoresponse-Wavelength measurements:

From the I–V measurements under illumination for different incident wavelengths, photoresponse – wavelength characteristics of a photodetector is measured and used to evaluate various performance parameters including responsivity, specific detectivity, external quantum efficiency (EQE), and transient response. The wavelength of the monochromatic light is varied across specified range (UV-Vis-IR) and corresponding photocurrent is recorded for every incident wavelength of light. The complete measurement setup used in our thesis work for photocurrent-wavelength characterization is shown in **Figure 1.12**.

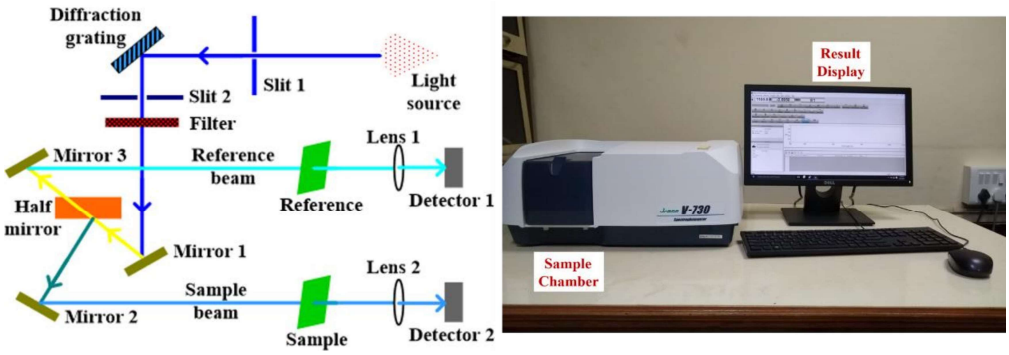


**Figure 1.10** Working mechanism and experimental setup used for UV-Vis Spectroscopy measurement.

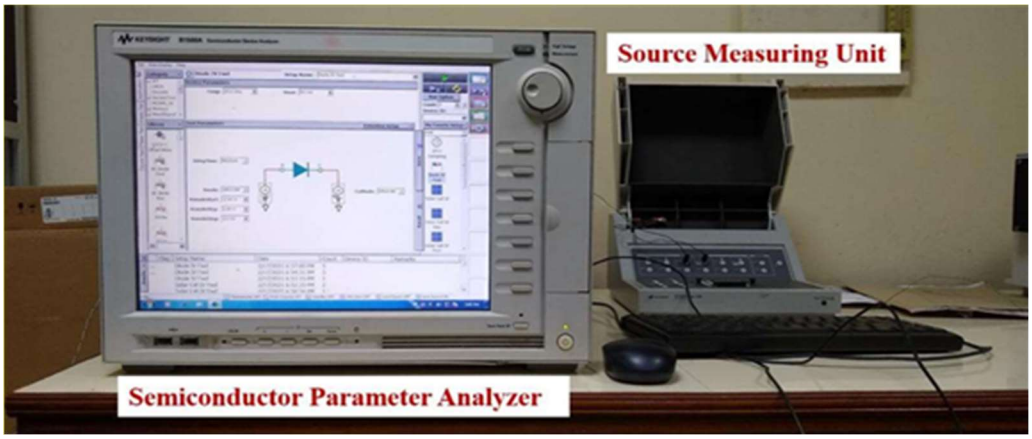


**Figure 1.11** Measurement setup using Semiconductor Parameter Analyzer and SMU for I-V characterization

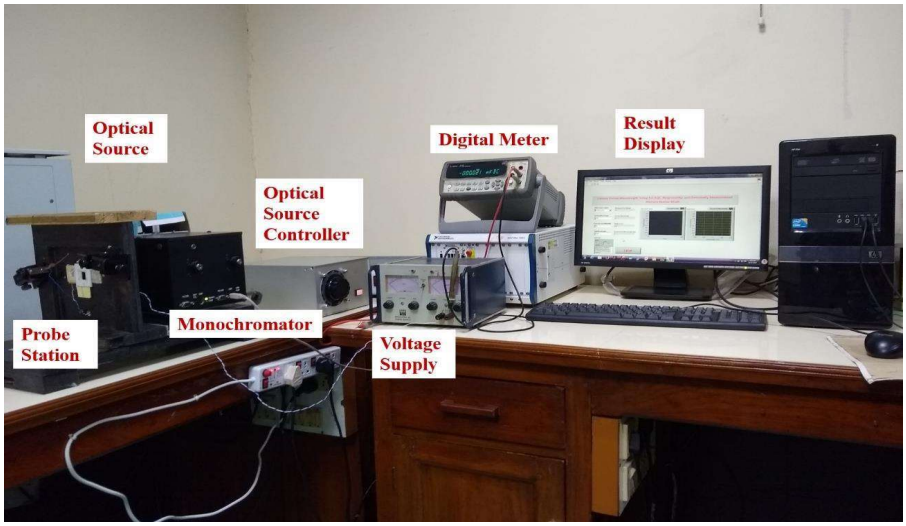


**Figure 1.12** Experimental setup for photocurrent-wavelength measurements to evaluate responsivity, specific detectivity, EQE and transient response of the fabricated device

Various instruments used for fabrication and characterizations of the thin film photodetectors considered in this thesis are shown in **Figure 1.13**

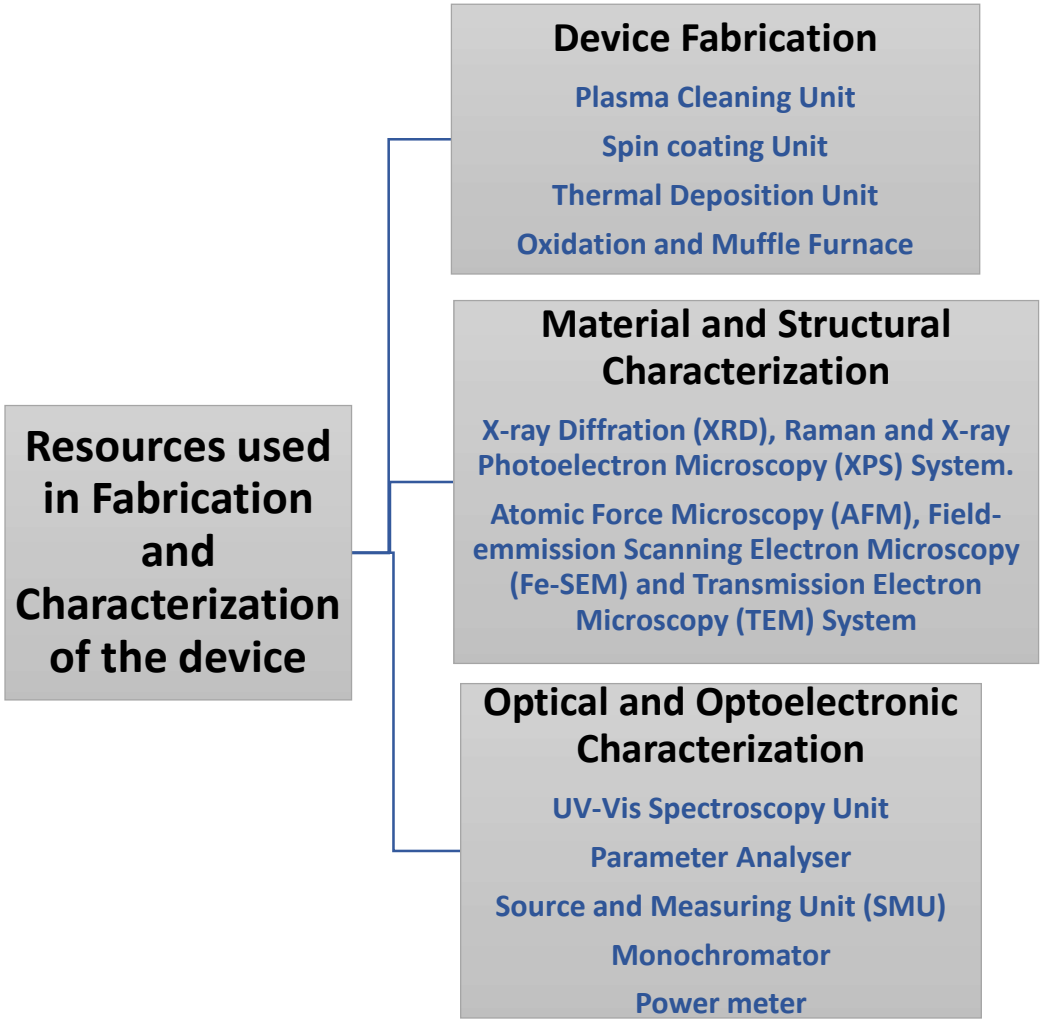


**Figure 1.13** Resources used in the Fabrication and Characterization of the device.

## 1.8 Literature Review on Transition Metal Dichalcogenides (TMDs)

Transition Metal Dichalcogenides (TMDs) have been known for decades, with a rich history and significant contributions to modern technological development. In the 1960s, during

early investigations, bulk TMDs such as $MoS_2$, $WS_2$, $MoSe_2$, and $WSe_2$ were synthesized and studied for their distinctive layered structures and catalytic properties [51]. Later, in the 1970s, researchers began exploring their potential applications in catalysis and lubrication, particularly in petroleum refining processes [51]. During the 1980s and 1990s, Russell R. Chianelli and colleagues reported the formation of tubular $MoS_2$ structures for potential catalytic applications [3]. However, in the 1990s and early 2000s, TMDs (including $MoSe_2$) remained niche materials with limited use in lubrication and electrochemical applications, largely due to the rise of other semiconducting materials such as Si, GaAs, and GaN [5].

In 2004, interest in TMDs was reignited following the discovery of graphene—the first two-dimensional (2D) material—by Andre Geim and Konstantin Novoselov, who were later awarded the Nobel Prize in 2010. The isolation of graphene through mechanical exfoliation inspired researchers to explore other 2D materials, with TMDs emerging as significant members of this new material family [43], [51].

The mechanical exfoliation of TMDs such as $MoS_2$, $WS_2$, and $MoSe_2$ was the initial method to isolate their monolayers. A significant property that made these materials ideal for optoelectronic applications was the indirect-to-direct bandgap transition when scaling from bulk to monolayer [43], [50], [51]. After 2010, scalable methods like Chemical Vapor Deposition (CVD) and Metal-Organic Chemical Vapor Deposition (MOCVD) were developed for synthesizing high-quality monolayer TMDs [62], [66], [77].Concurrently, studies expanded into doping, phase engineering, and the formation of heterostructures, enhancing their applicability in electronics and optoelectronics [58], [78]–[82]. While $MoS_2$

was extensively studied, $MoSe_2$, despite being comparatively underexplored, exhibited several advantages in device performance [47], [57], [59], [63], [66], [83]. The following summary highlights some key advances in $MoSe_2$-based photodetectors.

In 2013, Y. Zhang et al. [55] provided the first direct evidence of the bandgap transition in $MoSe_2$ via angle-resolved photoemission spectroscopy on MBE-grown thin films. In 2014, J. Xia et al. [77] synthesized large-area monolayer $MoSe_2$ via CVD and achieved a photoresponsivity of ~13 mA/W with a fast response (~60 ms) under 532 nm illumination. X. Wang et al. [62] also used CVD to grow monolayer $MoSe_2$ and demonstrated n-type FETs with ~50 $cm^2/V{\cdot}s$ mobility and ON/OFF ratio of ~$10^6$. Y. Chang et al. [66] reported high-quality CVD-grown $MoSe_2$ with fewer defects and ultrafast response (<25 ms). In contrast, C. Fan et al. [84] synthesized $MoSe_2$ flower-like nanostructures hydrothermally, showing slower but significant photoresponse (~7.89 s rise time).

In 2015, P. Rivera et al. [85] explored interlayer excitons in $MoSe_2/WSe_2$ heterostructures, showing strong tunable light-matter interactions using vertical gating. In 2016, Y. Hang et al. [67] fabricated trilayer $MoSe_2$ photodetectors via exfoliation with photoresponsivity of 26.2 mA/W and EQE of 5.1%. That same year, Li Xufan et al. [86] grew $GaSe/MoSe_2$ heterostructures via two-step CVD, demonstrating photovoltaic p–n junctions with ~30 mA/W responsivity. Also in 2016, J. Mao et al. [64] reported a $MoSe_2/Si$ heterojunction photodetector using graphene as the electrode with ultrafast response (270/350 ns) and detectivity of $7.13\times10^{10}$ Jones. In 2017, X. Chen et. al. [87] grew lateral heterojunction film of high-quality mosaic $MoS_2/MoSe_2$ on $SiO_2/Si$ substrate by chemical vapour deposition

(CVD) technique with responsivity, detectivity and EQE of 1.3 A/W, $2.6\times10^{11}$ Jones and 263.1 % respectively.

In 2018, H. Lee et al. [63] built a high-performance exfoliated $MoSe_2$ phototransistor, achieving responsivity of $1.4\times10^5$ A/W, detectivity of $5.5\times10^{13}$ Jones, and sub-3 ms response time. In 2019, M. Blauth et al. [57] demonstrated deep-subwavelength $MoSe_2$ photodetection using plasmonic waveguides, while B. Liu et al. [83] fabricated a self-powered graphene/$MoSe_2$/Au photodetector with 89.5 mA/W responsivity and 9.6 ms response time. T. Yang et al. [82] demonstrated broadband photodetection using $Bi_2O_2Se/MoSe_2$ heterostructures, achieving 413.1 mA/W responsivity and 0.79 s response time.

In 2020, Wen Du et al. [61] developed a near-perfect $MoSe_2$ absorber (99.5% at 686 nm) using polymer-assisted deposition, yielding an ON/OFF ratio of 729. V. Selamneni et al. [56] demonstrated a flexible $MoSe_2$/cellulose paper photodetector for NIR detection (780 nm) with robust bending stability. Later, C. Zankat et al. [80] built a self-powered $SnSe_2/MoSe_2$ heterostructure with high responsivity (7.09 A/W), detectivity ($6.44\times10^{12}$ Jones), and EQE (1313%).

In 2021, M. Hussain et al. [88] demonstrated a GeSe/$MoSe_2$ heterojunction p–n diode with 465 mA/W responsivity and tunable rectification, showing fast NIR response (850 nm). J. Duan et al. [78] developed $MoSe_2/FePS_3$ self-powered photodetectors, achieving 52 mA/W responsivity under ambient conditions. J. Chen et al. [89] reported ultrafast $MoSe_2$-$WSe_2$ p–n heterojunctions via CVD with 20 A/W responsivity and sub-35 μs response. H. Sandhu et al. [90] demonstrated a $MoSe_2$/n-GaN heterojunction for UV–NIR detection with a remarkable responsivity of 5580 A/W and gain of $1.8\times10^4$. Most recently, in 2024, X. Zhou

et al. [91] developed a $MoSe_2$/AgInGaS QD hybrid photodetector with enhanced detectivity ($6.4\times10^{11}$ Jones) and responsivity (14.3 A/W), showing over threefold improvement compared to standalone $MoSe_2$ devices.

The ZnO and transition metal dichalcogenides (TMDs) heterostructures have emerged as complementary materials for broadband photodetectors due to their synergistic optoelectronic properties. ZnO, a wide bandgap semiconductor (~3.3 eV), is highly responsive to ultraviolet (UV) light, while TMDs such as $MoS_2$, $MoSe_2$, and $WSe_2$ offer tunable bandgaps ranging from visible to near-infrared (NIR) regions in their monolayer or few-layer forms. When combined in heterojunction architectures, typically type-II band alignment is formed, facilitating efficient charge separation and broadband photodetection. For instance, Wan et al. demonstrated a self-powered $MoSe_2$/ZnO photodiode exhibiting ultrafast response (~40 μs), high responsivity (2.7 A/W), and broadband detection from UV to NIR, owing to the sharp atomically aligned n–n junction interface and efficient carrier transport across the heterojunction [58]. Similarly, Kang et al. fabricated a flexible $MoS_2$/ZnO hybrid photodetector using atomic layer deposition (ALD), achieving broadband detection with excellent responsivity and mechanical robustness [92]. Hybrid structures integrating ZnO quantum dots with $MoSe_2$ have also shown enhanced UV absorption and photogain due to improved light harvesting and charge transfer dynamics [93]. These advancements illustrate that ZnO/TMD heterostructures hold significant promise for high-performance, broadband, self-powered, and flexible photodetectors suitable for next-generation optoelectronic applications.

## 1.9 Thesis Motivation

Transition Metal Dichalcogenides (TMDs) have garnered considerable attention for their potential applications in quantum computing, flexible electronics, optoelectronics, and related fields [43], [50], [51]. Their thickness-dependent bandgap tunability makes them particularly attractive for designing photodetectors that operate across a wide range of wavelengths [43], [50], [51]. TMD-based broadband photodetectors have been extensively investigated [6], [60], [64], [82], [94]. Furthermore, TMD/ZnO heterostructure photodetectors offer an extended spectral response, covering the UV-Vis or UV-Vis-NIR regions [6], [58], [68], [92], [95]–[97]. Among the TMD family, $MoS_2$ is the most widely studied material, while $MoSe_2$ remains relatively underexplored for broadband photodetection. Nevertheless, $MoSe_2$ and ZnO/$MoSe_2$ heterostructures present significant opportunities for broadband photodetector applications due to $MoSe_2$'s higher electrical conductivity and light absorption capacity [73], greater carrier mobility [62], superior photodetection responsivity [63], faster response times [66], and enhanced photocatalytic activity [46], [49] compared to $MoS_2$.

The literature survey indicates that both the traditional mechanical exfoliation method [58], [67] and more sophisticated, expensive techniques such as Chemical Vapor Deposition (CVD) and Molecular Beam Epitaxy (MBE) [55], [64], [66], [77] have been employed to fabricate $MoSe_2$-based devices. While mechanical exfoliation is the simplest approach to isolate thin films or nanoflakes of 2D materials (including $MoSe_2$), it lacks scalability, offers low yield, and results in films with non-uniform and uncontrolled thickness. On the other

hand, thin film deposition using CVD or MBE, although capable of producing high-quality films, is costly and requires complex setups with high-temperature processing. Therefore, there is a compelling opportunity to explore simple and cost-effective methods such as vacuum thermal evaporation to achieve uniform TMD thin films with controlled thickness. In the present thesis, a low-cost and facile hydrothermal route has been used to synthesize $MoSe_2$ powder, which is subsequently deposited via thermal evaporation to form $MoSe_2$ thin films. There is also an opportunity to investigate the performance of $MoSe_2$/ZnO CQDs heterostructure-based broadband photodetectors using hot injection method for ZnO CQDs synthesis and its thin films fabrication using the low-cost spin coating technique.

## 1.10 Thesis Objective

The major objectives of this thesis are:

- To adopt a facile, low-temperature, and cost-effective hydrothermal route for the synthesis of the active material $MoSe_2$.
- To explore a simple and economical thermal evaporation method for $MoSe_2$ thin film deposition.
- To study thermally grown $MoSe_2$ thin film-based Metal–Semiconductor–Metal (MSM) broadband photodetectors.
- To fabricate and characterize n-$MoSe_2$/p-Si-based broadband photodetectors.

- To investigate $MoSe_2$/ZnO CQD-based n–n heterojunctions for high-performance broadband photodetection by synthesizing ZnO CQDs via the hot injection method and fabricating their thin films using the spin coating technique.

## 1.11 Organization of the Thesis

The present thesis aims to fabricate and characterize $MoSe_2$ thin film and $MoSe_2$/ZnO CQD heterostructure-based broadband photodetectors. Accordingly, the thesis is organized into five chapters, including the current chapter, which outlines the research motivation and objectives based on an extensive literature review. The remaining four chapters are summarized below:

**Chapter 2** investigates the performance of a thermally grown $MoSe_2$ thin film-based Metal–Semiconductor–Metal (MSM) broadband photodetector fabricated on a $SiO_2$-coated p-type Si substrate. $MoSe_2$ nanopowder was first synthesized via a facile hydrothermal route, and the $MoSe_2$ thin film was deposited using a cost-effective thermal evaporation technique. Interdigitated Ag Schottky contact electrodes were fabricated on the $MoSe_2$ thin film by thermal evaporation using the shadow masking technique. The morphological, electronic, and optoelectronic properties of the $MoSe_2$ film were studied in detail. Finally, the I–V characteristics of the proposed MSM photodetector were measured under dark and illuminated conditions to evaluate various performance parameters such as responsivity, detectivity, external quantum efficiency (EQE), and transient response.

**Chapter 3** presents the design and performance analysis of an Ag/n-$MoSe_2$/p-Si/Al broadband photodetector, where the n-$MoSe_2$/p-Si heterojunction was formed by depositing $MoSe_2$ on a p-Si substrate via thermal evaporation. The $MoSe_2$ nanopowder synthesized by the hydrothermal method, as described in Chapter 2, was used here as well. For electrical contacts, circular Ag metal dots were deposited on the $MoSe_2$ film and an Al layer was deposited on the backside of the Si substrate by thermal evaporation. The electronic and optoelectronic properties of the $MoSe_2$ film were thoroughly investigated. I–V measurements were performed under dark and illuminated conditions to determine the photodetector's performance metrics.

**Chapter 4** explores the performance of a ZnO CQD/$MoSe_2$-based n–n heterojunction UV–Visible broadband photodetector. The device was fabricated on an indium tin oxide (ITO)-coated glass substrate. ZnO CQDs synthesized by the hot injection method were spin-coated onto the substrate, and $MoSe_2$ nanopowder synthesized by the hydrothermal method was deposited on top of the ZnO CQD layer via thermal evaporation. The thin film and device characterizations were carried out using similar methodologies as in the previous chapters.

**Chapter 5** summarizes the major findings of the thesis and outlines potential directions for future research in the field of $MoSe_2$-based broadband photodetectors.